Fractional-length sync-pumped degenerate optical parametric oscillator for 500-MHz 3-μm mid-infrared frequency comb generation

Kirk A. Ingold,[1,*] Alireza Marandi,[1] Charles W. Rudy,[1] Konstantin L. Vodopyanov,[1,2] and Robert L. Byer[1]

[1]*E. L. Ginzton Lab, Stanford University, Stanford, California 94305, USA*

[2]*CREOL, College of Optics & Photonics, University of Central Florida, Orlando, Florida 32816, USA*

**Corresponding author: kaingold@stanford.edu*

Received December 3, 2013; accepted December 22, 2013;
posted January 6, 2014 (Doc. ID 202507); published February 10, 2014

We demonstrate a mid-IR frequency comb centered at 3120 nm with 650-nm (20-THz) bandwidth at a comb-teeth spacing of 500 MHz. The generated comb is based on a compact ring-type synchronously pumped optical parametric oscillator (SPOPO) operating at degeneracy and pumped by a mode-locked Er-doped 1560 nm fiber laser at a repetition rate of 100 MHz. We achieve high-repetition rate by using a fractional-length cavity with a roundtrip length of 60 cm, which is one-fifth of the length dictated by conventional synchronous pumping.

OCIS codes: (190.4970) Parametric oscillators and amplifiers; (190.7110) Ultrafast nonlinear optics.
http://dx.doi.org/10.1364/OL.39.000900

Frequency combs with large comb spacings are useful in applications such as precision spectroscopy [1,2], astronomical spectrograph calibration [3,4], and optical arbitrary waveform generation [5]. These sources are well established in the visible and near-infrared spectral regions, but are less developed in the mid-infrared.

We have shown previously that degenerate synchronously pumped optical parametric oscillators (SPOPOs) are efficient tools to transfer near-IR frequency combs to the mid-IR [6,7]. They benefit from large instantaneous bandwidth, low threshold, and high conversion efficiency. However, the SPOPO repetition rate was limited by the pump (≤100 MHz). It also has been shown that the frequency comb salient features, such as carrier envelope offset and repetition rate, are transferred to the mid-IR at degeneracy [8]. Thus, using a high repetition rate near-IR source, SPOPOs show promise for extending the mentioned applications into the mid-IR [9].

Well-established techniques to achieve a comb spacing >1 GHz in the near-IR currently are based on spectrally filtering lower repetition rate frequency comb sources [2,3,10]. These methods use a Fabry–Perot cavity with a large free spectral range (FSR) to increase the separation between comb lines while preserving the initial spectral envelope.

In singly resonant SPOPOs, using a cavity with an FSR equal to an integer of the pump repetition rate has effectively generated output pulses at higher repetition rates [11–14]. A similar technique using a fractional increase of the cavity roundtrip has been used in a singly resonant SPOPO with the signal wavelength in the near-IR [15].

In this Letter, we demonstrate a compact degenerate SPOPO to generate a high-repetition rate broadband mid-IR frequency comb centered at 3120 nm. It is built around a cavity with an FSR that is five times the repetition rate of the pump.

Figure 1 schematically shows the degenerate high-repetition rate SPOPO. The ring resonator is similar to that reported in [6,8]; however, the roundtrip length is 60 cm, corresponding to the 5th harmonic of the pump repetition frequency. The SPOPO is pumped with a mode-locked Er-doped fiber laser, which produces ~70 fs (Gaussian) pulses at a 100 MHz repetition rate. The center wavelength of the pump laser (λ_p) is 1560 nm, and the maximum average pump power is 250 mW.

The pump input coupler, mirror M_1, is a flat dielectric mirror designed for a high transmission ($T > 96\%$) for the pump beam and high reflectivity ($R > 97.5\%$) between 2600 and 4100 nm. Mirrors M_2 and M_3 are gold coated ($R > 98\%$) and concave with a radius of curvature $R = 25$ mm. Mirror M_4 is flat.

Broadband gain centered around 3120 nm is provided by a short, 1 mm long MgO-doped periodically poled lithium niobate (MgO:PPLN) crystal (Crystal Technologies Inc.). The crystal was designed for type-0 ($e + e \rightarrow e$) phase-matched subharmonic generation (at 32°C) with a quasi-phase matching period of 34.8 μm [6,8]. Mirror M_1 was designed to provide dispersion compensation (up to the 3rd order) for a 1 mm long piece of PPLN at the signal wavelength (GDD of 1-mm PPLN ~ – 575 fs^2

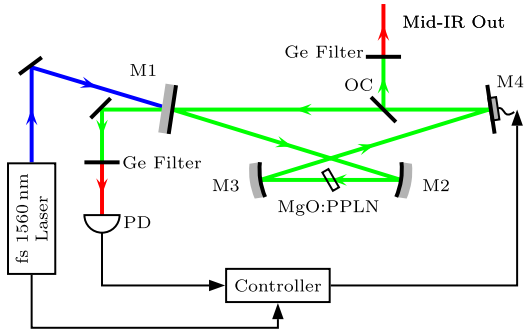

Fig. 1. Schematic of the fractional-length degenerate SPOPO. M_2 and M_3 are concave mirrors, and M_1 and M_4 are flat mirrors. The output coupler (OC) is a pellicle beamsplitter. An InAs photodetector (PD) is located after a Ge long pass filter (>2.5 μm). The blue beam represents near-IR (1.56 μm). The red beam represents the mid-IR (3.12 μm). The green beam represents the overlap of the near-IR and mid-IR.

at 3120 nm). The output coupler (OC) is an uncoated 2 μm thick pellicle beam splitter oriented to provide ~2% output coupling at the signal wavelength. Leakage through mirror M_1 was used for diagnostics and to stabilize the cavity length to maximize the output power.

The PPLN crystal was cut at the Brewster angle for the signal wavelength to reduce losses. To compensate for the astigmatism introduced by the angled crystal, we chose a 7° angle of incidence for mirrors, M_2 and M_3, which minimized the intracavity astigmatism. These mirrors were chosen to have a small radius of curvature to tightly focus the pump/signal and increase the parametric gain in the system. The separation between these mirrors was set such that the $1/e^2$ waist size of the signal beam is ~16 μm inside the crystal.

Typical of degenerate SPOPOs, we achieved oscillation at discrete cavity lengths [6], which we identify as oscillation peaks. As Fig. 2 shows, these oscillation peaks were spaced at intervals of ~312 nm or $\lambda_p/5$. In Fig. 2(a), we show the SPOPO spectrum as a function of the roundtrip cavity length. The spectrum was measured through the dichroic mirror, M_1. This figure shows that the SPOPO operates at degeneracy across all of the oscillation peaks, which suggests the dispersion of the PPLN is well compensated by the chirped mirror.

We observed the lowest pump threshold without the pellicle OC in the cavity at ~40 mW. After inserting and optimizing the angle of the pellicle in the cavity for maximum output power of the signal, the threshold increased to ~125 mW. The number of distinct cavity lengths where oscillation occurred reduced to three in this case, as Fig. 2(b) shows. We attribute this change to the increase in loss and increased pump threshold due to the OC.

We also stabilized the cavity length at each individual oscillation peak with a "dither-and-lock" method [8] and measured the output spectrum using a grating-based monochromator. Each oscillation peak exhibited degenerate behavior where the signal and idler spectra overlap. The dither-and-lock circuit had a corner frequency of 10 Hz, which was adequate to lock the cavity length to a desired peak for several hours. For the results presented in the remainder of the Letter, we locked the cavity on the peak that generated the highest output power, represented by Peak 1 in Fig. 2(b).

The maximum achieved output power of the signal in this configuration was ~8.5 mW when pumped with 250 mW. Using a fast InAs photodetector (PD), we recorded the 500 MHz signal pulse train, as shown in

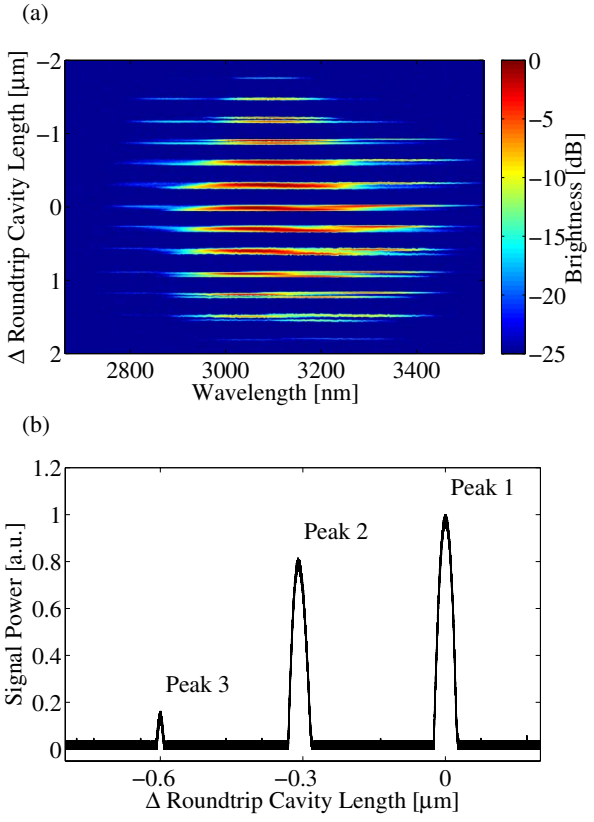

Fig. 2. (a) Measured output spectrum as the cavity length is swept. The output of the SPOPO was measured through mirror, M_1. The SPOPO oscillates at several discrete cavity lengths. (b) Oscillation peaks observed when a pellicle beamsplitter is used as an OC. The number of peaks is reduced to three and they are separated by 312 nm or $\lambda_p/5$.

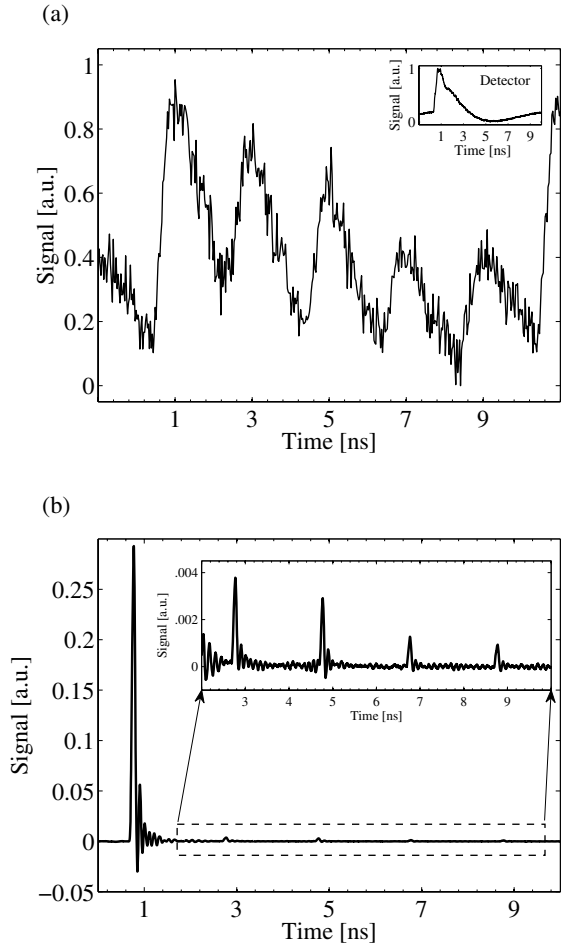

Fig. 3. (a) Output pulse train of the 500-MHz repetition rate SPOPO at a signal wavelength of 3120 nm. (Inset) Detector response of a 100 MHz 1560 nm pulse train. (b) The SHG 1560 nm output of the SPOPO is shown. Significant residual pump is seen in the first pulse located at 1 ns. The inset shows a close up of pulses 2–5, which are not present when the SPOPO is not oscillating.

Fig. 3(a). The 100 MHz amplitude modulation in the pulse train is expected due to the low finesse of the cavity and the existence of parametric gain created by the pump pulses only coinciding with every fifth roundtrip of the signal.

The InAs detector was loaded with a 1 – Ω resistor to decrease the RC-time constant and enable us to measure the pulses and the 500 MHz repetition rate. We expected to see an exponential decay of the intensity of pulses over the four periods where the pump and signal pulses trains did not overlap. As shown in Fig. 3(a), the nonideal exponential decay in the measured pulse train is due to the response of the detector circuit. We confirmed the detector response by measuring only the 100-MHz pump pulses on the InAs detector when the SPOPO was not oscillating [see Fig. 3(a) inset].

For signal pulses that do not overlap with the pump, the nonlinear crystal is phase matched for second harmonic generation (SHG). This process can act as a nonlinear loss mechanism in the SPOPO. The effect depends on the peak power of the pulses in the cavity, and therefore, we expected that a change in the out coupling would have an additional small nonlinear effect on the temporal decay of the signal pulses.

Using a fast extended InGaAs PD (Newport 818-BB-51 detector with a 12.5 GHz response), we recorded the output of the SPOPO when it was oscillating. We observed the 1560 nm pulses from SHG of the intracavity 3120 nm signal, as shown in Fig. 3(b). Taking into account that the intracavity 3120 nm signal scales as the square root of this detected second harmonic at 1560 nm and comparing the pulse-to-pulse ratio of pulses 3–4 and pulses 4–5, we estimated the cavity losses for the 3120-nm signal change from 29% (pulse 3 → 4) to 15% (pulse 4 → 5). This confirmed the existence of a nonlinear loss mechanism in the cavity. Further studies of this effect is beyond the scope of this Letter.

The output spectrum was captured using a grating-based monochromator and a TE-cooled InSb detector. The results are shown in Fig. 4(a). The measured 3-dB bandwidth is 144 nm. A bandwidth of 650 nm (20 THz) was recorded at the detector noise floor of –35 dB, suggesting this source is suitable for applications in spectroscopy.

The interferometric autocorrelation of the signal pulses in Fig. 4(b) shows slightly chirped pulses with an autocorrelation width of 197 fs. To estimate the SPOPO pulse length, we numerically fit a spectral phase to the measured spectrum to match the measured autocorrelation. Then, we numerically compensated for the 3 mm thick Ge filter in the measurement (GDD ~4300 fs^2) and calculated the approximate pulse width of the signal pulses before the Ge filter to be 109 fs. The transform-limited pulse length for a 144 nm bandwidth is 99 fs for a Gaussian pulse. We expected a slight difference in temporal pulse shape of each of the five decaying pulses due to additional dispersion from multiple roundtrips in the cavity because the dispersion compensating mirror is not perfect; therefore, this is effectively a measurement of the average pulse duration.

This fractional-length degenerate SPOPO not only increases the repetition rate of the output pulse train, but also the compact cavity design could reduce some

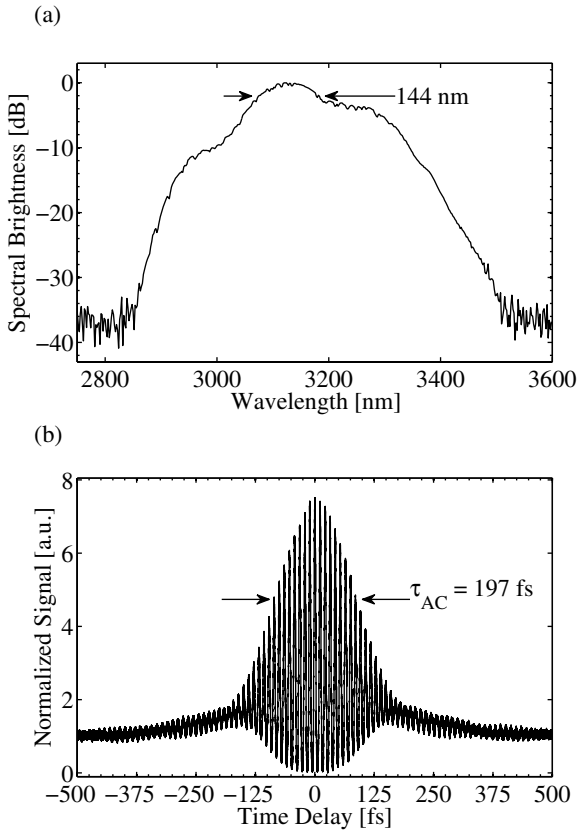

Fig. 4. (a) Optical spectrum of the SPOPO output with 8.5 mW average power. The –3 dB bandwidth is approximately 144 nm. Additionally the spectrum covers a 650 nm (20 THz) bandwidth at –35 dB. (b) Measured interferometric autocorrelation of the 500 MHz pulse train with 8.5-mW average power. The trace suggests the pulse length at the output of the SPOPO is 109 fs.

of the practical limitations of using degenerate SPOPOs without compromising performance. The small size of the cavity reduced the vulnerability to environmental noise. These benefits allow for a degenerate SPOPO to be used more easily for intracavity molecular spectroscopy [16], where we expect the compact SPOPO would provide similar intracavity absorption enhancement while requiring $1/N$ of the length (where N is the repetition rate multiplier).

In summary, we have demonstrated a compact degenerate SPOPO using a ring cavity with a fractional length of the conventional SPOPO cavity length to produce a comb that spans 2850–3500 nm with a repetition rate of 500 MHz from a commercially available 100 MHz near-IR frequency comb source. The compact size and higher repetition rate makes this SPOPO appealing for many mid-IR frequency comb applications. By further reducing the cavity length and cavity losses or increasing the pump power, the comb spacing can be extended beyond >1 GHz.

The authors thank Vladimir Pervak and the German Research Foundation Cluster of Excellence “Munich Centre for Advanced Photonics.” We gratefully acknowledge support from the U.S. Office of Naval Research and The National Aeronautics and Space Administration (NASA).

References

1. M. Thorpe and J. Ye, Appl. Phys. B **91**, 397 (2008).
2. S. A. Diddams, L. Hollberg, and V. Mbele, Nature **445**, 627 (2007).
3. C. H. Li, A. J. Benedick, P. Fendel, A. G. Glenday, F. X. Kartner, D. F. Phillips, D. Sasselov, A. Szent-Györgyi, and R. L. Walsworth, Nature **452**, 610 (2008).
4. T. Steinmetz, T. Wilken, C. Araujo-Hauck, R. Holzwarth, T. W. Hänsch, and T. Udem, Appl. Phys. B **96**, 251 (2009).
5. S. T. Cundiff and A. M. Weiner, Nat. Photonics **4**, 760 (2010).
6. N. Leindecker, A. Marandi, R. L. Byer, and K. L. Vodopyanov, Opt. Express **19**, 6296 (2011).
7. C. W. Rudy, A. Marandi, K. A. Ingold, S. J. Wolf, K. L. Vodopyanov, R. L. Byer, L. Yang, P. Wan, and J. Liu, Opt. Express **20**, 27589 (2012).
8. A. Marandi, N. C. Leindecker, V. Pervak, R. L. Byer, and K. L. Vodopyanov, Opt. Express **20**, 7255 (2012).
9. M. Vainio, M. Merimaa, L. Halonen, and K. L. Vodopyanov, Opt. Lett. **37**, 4561 (2012).
10. M. S. Kirchner, D. A. Braje, T. M. Fortier, A. M. Weiner, L. Hollberg, and S. A. Diddams, Opt. Lett. **34**, 872 (2009).
11. D. T. Reid, C. McGowan, W. Sleat, M. Ebrahimzadeh, and W. Sibbett, Opt. Lett. **22**, 525 (1997).
12. B. Ruffing, A. Nebel, and R. Wallenstein, Appl. Phys. B **67**, 537 (1998).
13. J. Jiang and T. Hasama, Opt. Commun. **211**, 295 (2002).
14. P. J. Phillips, S. Das, and M. Ebrahimzadeh, Appl. Phys. Lett. **77**, 469 (2000).
15. A. Esteban-Martin, O. Kokabee, K. Moutzouris, and M. Ebrahimzadeh, Opt. Lett. **34**, 428 (2009).
16. M. W. Haakestad, T. P. Lamour, N. Leindecker, A. Marandi, and K. L. Vodopyanov, J. Opt. Soc. Am. B **30**, 631 (2013).